J. Phys. Chem. Solids Pergamon Press 1968. Vol. 29, pp. 1177–1189. Printed in Great Britain.

X-RAY OBSERVATION OF CHEMICAL AND POLYMORPHIC EQUILIBRIA UNDER HYDROSTATIC PRESSURES

BRIANT L. DAVIS

Institute of Atmospheric Sciences, South Dakota School of Mines and Technology, Rapid City, South Dakota, U.S.A.

and

MICHAEL J. WALAWENDER*

Department of Geology and Geological Engineering, South Dakota School of Mines and Technology, Rapid City, South Dakota, U.S.A.

(*Received* 28 *August* 1967; *in revised form* 19 *January* 1968)

Abstract—A pressure vessel has been designed for use with fluid pressures to 5000 bars and temperatures to 300°C in combination with X-ray diffraction examination *in situ*. A narrow X-ray beam is passed through the pressure fluid onto the sample contained within a beryllium cylinder, with pressure being developed by an 'O'-ringed piston.

Examination of various phases within the system $CaSO_4$–H_2O has revealed the existence of at least one, possibly more new phases, most likely hydrous, that appear to be stable only in the presence of low pressures (to 500 bars). One of these phases can be indexed on the basis of a distorted anhydrite cell with $a = 6{\cdot}46_9$ Å, $b = 6{\cdot}81_5$ Å, and $c = 7{\cdot}14_8$ Å ($Z = 4$). Gypsum in the presence of a 4 molal NaCl solution has been converted to the hemihydrate phase at 98 ± 2°C under 100 bars pressure, but no such conversion was observed using distilled water.

Investigation of the conditions of stability of AgI–IV with this vessel and with Van Valkenburg's high-pressure optical device has shown that (1) pure cubic (II′) or fine grained mixtures of cubic and hexagonal (II) AgI cannot be completely converted to phase IV within the times allotted, (2) pure hexagonal AgI (II) can be quickly converted to phase IV without polygonization, and (3) the II–III phase boundary is essentially correct as originally determined by Bridgman in 1915.

1. INTRODUCTION

MOST chemical data pertaining to solid-liquid equilibria, as well as certain polymorphic transformations, must be obtained indirectly by means of volume changes, electrical resistivity, or a number of indirect analytical techniques. In most of these instances observation of composition and structure of the resulting solid products is made after the reaction or inversion is complete. Such observations yield results that are usually assumed to pertain to equilibrium conditions, or at least to conditions that existed during formation of the solid product. For example, the formation of AgI from addition of a potassium iodide solution to a silver nitrate solution appears to result in mixtures of both the hexagonal and cubic type of AgI, or at least it so appears after the filtering, washing and drying processes carried out prior to X-ray examination. X-ray examination during formation *in situ* would not only eliminate this uncertainty but the possible temporary existence of structurally distinct intermediate phases would also be ascertained.

An X-ray device is described below which permits examination of the solid phases involved in chemical or polymorphic processes while reaction and inversion is actually in process. Certain phase relationships in the $CaSO_4$–H_2O system, and a re-examination of a portion of the AgI phase diagram is presented here as the initial study using this apparatus.

**Present Address:* Department of Geochemistry and Mineralogy, Pennsylvania State University, University Park, Pennsylvania 16802, U.S.A.

2. X-RAY FLUID PRESSURE VESSEL

Vessels for the *in situ* study of polymorphic transformations under high pressure and temperature by means of X-rays have been in use several years (Klement and Jayaraman[1], p. 297). However, these vessels function only with nonhydrostatic to partially hydrostatic pressures except for certain vessels operating at high pressures (above 30,000 atm.). Brief mention was made by Adams and Davis[2] of an X-ray vessel using fluid pressures, but no description was given. The present device differs from the one mentioned by Adams and Davis in that the pressure range is slightly lower but the life of the bomb is considerably increased. The present device is considerably less expensive to operate.

Figure 1 is a drawing at half natural size of the present X-ray vessel. The vessel consists of three main parts; a central beryllium cylinder drilled with a 0·180 in. hole to a depth of two-thirds of the cylinder height; a tool-steel (No. 4340, Solar, or No. 883) upper support jacket into which the beryllium cylinder is forced (with about 0·002 in. interference); and a lower jacket that can be screwed onto the upper assembly with sufficient force to apply considerable end-load support. Without such support the beryllium cylinder fails on a surface slightly conical and concentric to the cylinder axis at about 3000 bars whereas with the end-load support pressures up to 4000 bars can be attained. The sample in the form of powder or pellet is placed at the bottom of the blind hole in the beryllium cylinder and several mm of appropriate pressure fluid placed above it. The pressure in the fluid is created by application of thrust from a single or double 'O' -ring piston above it. For polymorphic transformations, dehydration and decarbonation reactions, etc., an inert pressure fluid such as pentane or iso-pentane is used as the pressure fluid. For reactions involving active solutions, these solutions act as the pressure medium as well as part of the X-ray 'window'; or, if no pressure is desired the piston may be left out of the vessel and the top sealed by a number of methods.

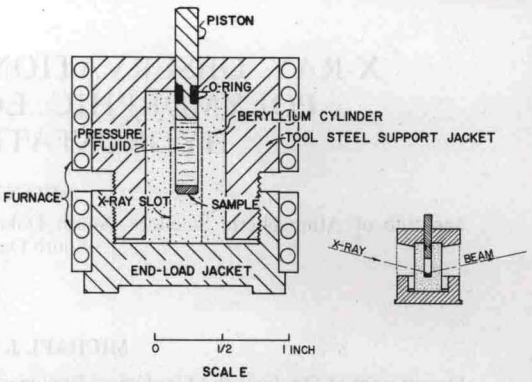

Fig. 1. Schematic diagram of X-ray fluid pressure vessel. Stippled portion is beryllium cylinder. Plane of small diagram (showing slots in support casing and X-ray path) is normal to that of large diagram.

A heating jacket surrounds the exterior of the vessel and is composed of No. 24 Brown and Sharpe nichrome heating element wrapped in fiber glass insulation. A chromel–alumel thermocouple is brought into one of the X-ray windows cut into the upper support jacket and contacts the beryllium cylinder approximately 1/4 in. from the sample. Although the vessel is capable of withstanding 500°C for several hrs (before oxidation of the cylinder requires its replacement) the 'O' -rings cannot maintain more than a few hundred bars pressure above 75°C.

The X-radiation used is restricted to molybdenum ($\lambda = 0{\cdot}7107$ Å), or one of even shorter wavelength. Considering both the beryllium cylinder thickness (0·625 in.) and bore thickness (0·180 in.), the absorption relation for the X-ray beam passing through the vessel is given by

$$\frac{I}{I_0} = \exp -\left[\left(\frac{\mu}{\rho}\right)\frac{\rho x}{\cos\theta}\right]_c \exp -\left[\left(\frac{\mu}{\rho}\right)\frac{\rho x}{\cos\theta}\right]_f \tag{1}$$

where I is the intensity of the emerging beam, I_0 is the initial beam intensity, (μ/ρ) is the mass absorption coefficient, ρ is the density, and x the diameters of the cylinder c, and pressure fluid f. At 0° 2θ with water pressure

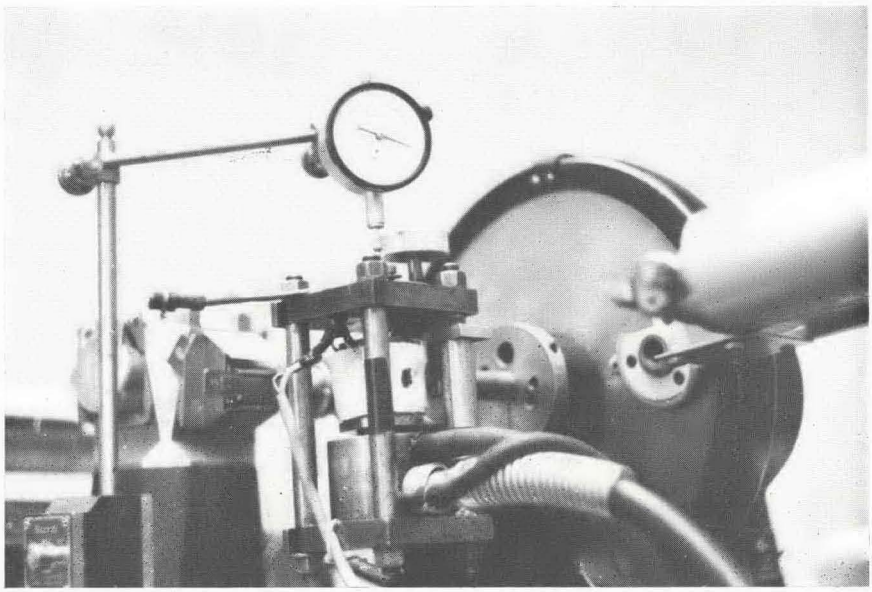

Fig. 2. X-ray vessel with press mounted in X-ray goniometer. Dial gauge at top is for sample height adjustment.

[*Facing page* 1178]

fluid the absorption of the X-ray beam is 62 per cent, and at 90° 2θ it is 84 per cent. Within the range of 5° to 30° 2θ necessary for most studies the resulting diffraction pattern is quite good, especially when scanning at 1/4 or 1/8 deg 2θ/min. The absorption is somewhat less when using pentane as a pressure fluid but the low angle diffraction ring (semi-coherent scatter) of such hydrocarbons makes reading of peaks in the 5–12° 2θ region more difficult.

Figure 1 also contains a small schematic diagram showing the X-ray slots and the beam path. The only unsupported portion of the vessel is that exposed in the jacket slots. Figure 2 shows the vessel and press mounted in a standard X-ray diffractometer.

Figure 3 presents the calibration data for pressures to 4000 atm., using a single 'O' -ring piston. One notes that the up pressure data show very little friction lag. The readings from the calibration curve are considered good to within $\pm 0{\cdot}10P$ where P is the internal pressure within the vessel. The data were obtained using potassium iodide with compression constants of Slater[3].

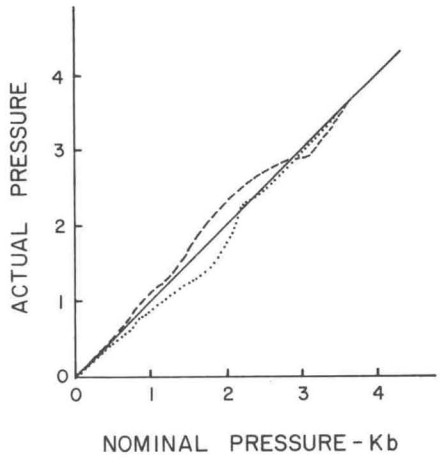

Fig. 3. Pressure calibration of vessel. Compression standard used was KI with pentane pressure fluid.

3. INVESTIGATIONS IN THE SYSTEM $CaSO_4$–H_2O

The literature pertaining to phase relations in the system $CaSO_4$–H_2O is both vast and confusing. No attempt is made here to review the contributions on the matter but the reader may refer to the summary in Deer *et al.*[4] (p. 202) and to Flörke[5] for fairly complete accounts. The primary interest in the present study was to look for structural changes in gypsum and anhydrite as a result of applied pressure and temperature. The new data presented here does not appear to clear up any of the questions regarding the identities of the hemihydrate, and γ–$CaSO_4$.

A. Effect of salinity on the gypsum–hemihydrate transformation

The hypsum–anhydrite transformation did not take place using distilled water at temperatures of 115°C for 12 hrs in the beryllium vessel. The phase described by Posnjak[6] as the hemihydrate was also not observed under these conditions. The piston was placed in the vessel during this experiment but the only pressure developed was that due to the vapor pressure of the super-heated H_2O above the sample. At this temperature this pressure is 25 bars, which would appear insignificant as far as altering the phase relationships is concerned. Thus, for the duration of the experiment, gypsum in pure water persisted metastably beyond the 42°C inversion for anhydrite and the 97°C inversion to the hemihydrate.

Similar experiments using gypsum as the starting material were performed using a 4 molal solution of NaCl. The transformation to anhydrite was again not possible for the several hour duration of the run; however, the gypsum was converted at 98 ± 1°C and 100 bars pressure to a phase which appears to be the hemihydrate as described by Posnjak[6]. The conversion time was about 1/2 hr but an incubation period of about 15 min above the 97°C transformation point was noted. Figure 4(A) and (B) are direct tracings of the diffractometer record for gypsum and the hemihydrate for the observed transformation *in situ*.

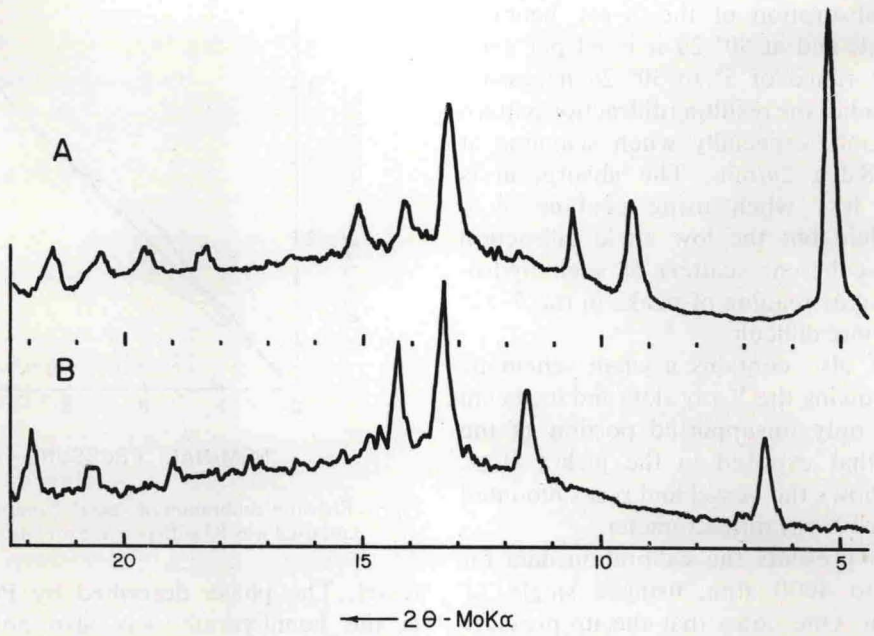

Fig. 4. (A) Diffraction record from X-ray vessel of $CaSO_4$–$2H_2O$ in distilled water at 26°C and atmospheric pressure. (B) Diffraction record from X-ray fluid pressure vessel of $CaSO_4 \cdot 1/2H_2O$ (Hemihydrate)formed from gypsum at 98 ± 2°C and 100 bars pressure in 4 molal NaCl solution.

The spacing and intensity data are given in Table 1.

B. Experiments with anhydrite + water under pressure

A large number of experiments were designed to observe the changes in X-ray pattern of anhydrite in the presence of water, with and without high pressures. Most experiments were carried out at room temperature in the beryllium cylinder under slight pressure, but one experiment was performed by scanning the standard powder 'well' mount with the powder material immersed in water.

In the 'well' mount experiment, as well as those using the cylinder with piston removed, a very pronounced variation with time of certain diffraction peaks of the anhydrite (notably the unresolved 020 + 002 doublet) was observed. In addition to this, certain weaker peaks would appear and disappear within 1/2 deg 2θ of this doublet. Figure 5 is a portion of an oscillation record showing

Table 1. *Interplanar spacings and intensities of* $CaSO_4 \cdot 1/2H_2O$ *formed at* 98 ± 1°C *and* 100 *bars from gypsum in beryllium vessel* *

d (Å)	I/I_0
6·04	32
3·46	33
3·01	100
2·81	47
2·75	10
2·14	10
1·85	30
1·48	5

*MoKα, 45 mV, 20 mA, 1/8 deg/min. scan speed, 1/4 divergence and scatter slits, 0·006 receiving slit.

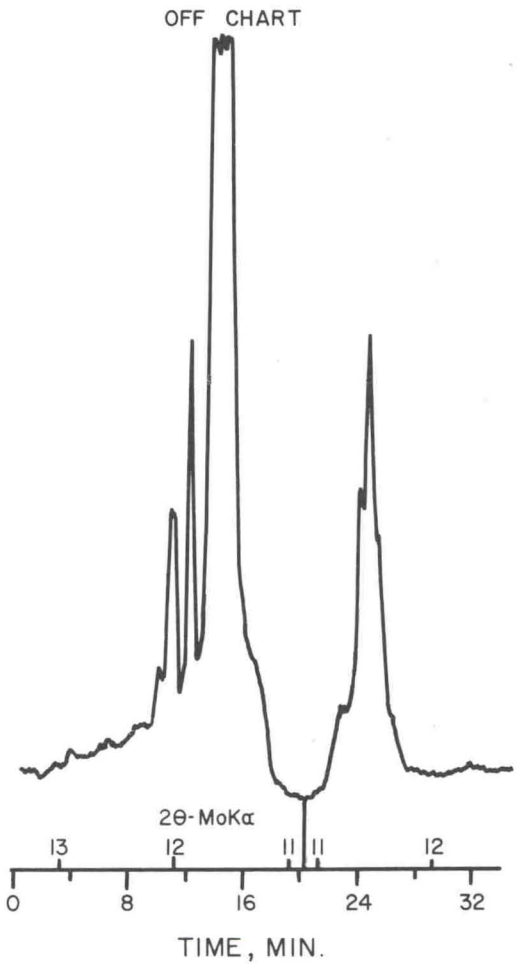

Fig. 5. Oscillation record taken at 1/4 deg 2θ per min in X-ray vessel of anhydrite in the presence of distilled water open to the atmosphere. Large peak at 11·5 deg 2θ is unresolved anhydrite 020–002 doublet.

variation in Bragg-angle and time with peak intensity. This figure shows both the extreme change in intensity of the 020–002 doublet of anhydrite and the momentary appearance of two other peaks whose interplanar spacings are smaller than those of the doublet.

Well over a dozen separate records of this type have been obtained, and in general the peaks that appear about the 020–002 doublet vary in position, although two peaks make an exception of this rule. These pertain to interplanar spacings of 3·57 and 3·61 Å and they usually are not resolved. The significance of these spacings will be discussed further below.

A meaningful demonstration of the intensity variability of the 3·50 Å spacing (020–002 doublet) of anhydrite is given by fixing the X-ray goniometer at the proper Bragg-angle and allowing the strip-chart recorder to run for several minutes. A 64 min record of this variation using the beryllium cylinder open to the atmosphere is presented as Fig. 6. One observes here that the changes persist over periods as long as 8 min (with minor variations); the longest period of increased intensity observed in 400 mins of recording time was 20 min.

In order for coherent diffraction to result from powder samples, in addition to complying with Bragg geometry, two other conditions must be met; (1) the sample must be sufficiently fine-grained to ensure large numbers of crystals of appropriate orientation for each spectral position, and (2) the grains must not be preferentially oriented. If either, or both, of these conditions are not met, the resulting diffraction pattern will show some or nearly all peaks absent. It appears that in the case of the 020–002 doublet one or both of these conditions are being met only part of the time. That is, there is continuous change in grain size and/or change in grain orientation. Such a phenomenon is best explained by the slight solubility of $CaSO_4$ in pure H_2O approximately 0·2 gm/100 ml at 30°C. It appears that we are here observing directly a chemical reorientation resulting from solution and precipitation that is continually going on in a solution at equilibrium. Since the vessel is not agitated, nor the temperature changed, there should be no cause for physical reorientation of the grains, or for chemical disequilibrium to develop.

The phenomenon of appearance of additional peaks in the region of the 020–002 doublet cannot be explained as a function of solubility. Such peaks point to the temporary formation of additional interplanar spacings

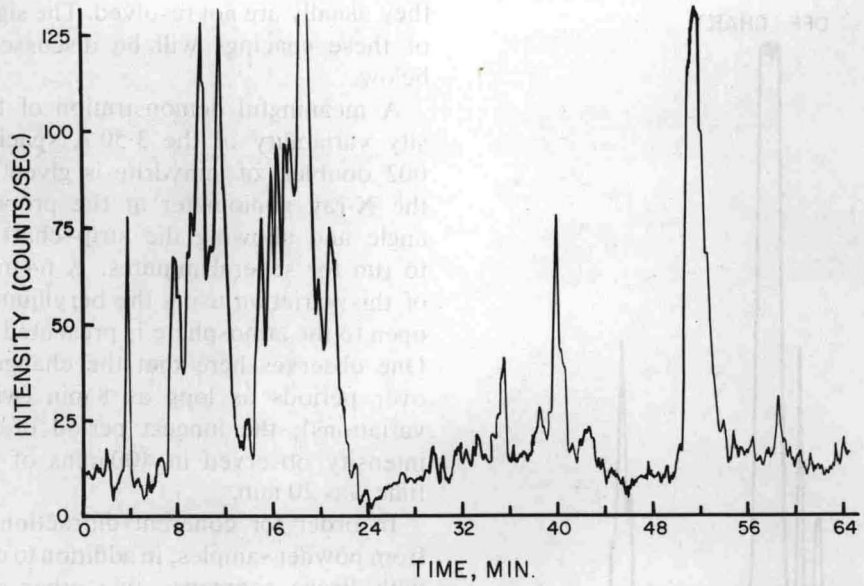

Fig. 6. Continuous time record of intensity variation of anhydrite 020–002 doublet in the presence of distilled water open to the atmosphere.

in the structure, whether it be by expansion of anhydrite spacings or by change in type or quantity of atoms comprising, or lying between a given spacing.

Additional experiments with anhydrite in the presence of water combined with pressures to 1000 bars revealed additional peaks in the pattern as well as elimination of certain anhydrite peaks. In particular the 3·57 and 3·61 Å spacings become stronger with the addition of slight pressures. There is apparently some conditioning of the sample necessary to produce certain of the observed peaks; it was found, for example, that raising the pressure to 300–500 bars and then reducing the pressure to near atmospheric produced the greatest changes in the anhydrite pattern. Figure 7 shows three diffractometer tracings of the changes observed. The standard pattern for anhydrite, but with weak development of the 3·57 and 3·61 Å spacings at about 11·4 deg. 2θ, is shown in Fig. 7(A). The pattern shown in Fig. 7(B) was produced from anhydrite having undergone the cycle mentioned above with the exception that the pressure was again raised to 200 bars (with no change in pattern). Figure 7(C) is a pattern from the same sample taken at a pressure of 50 bars. The greatest differences in comparison to the anhydrite pattern are indicated in this run and it is apparent that a completely different phase of $CaSO_4$ (undoubtedly partially hydrated) is present.

Table 2 presents the observed spacing and intensity data measured from the patterns of Fig. 7(B) and (C). Some of the spacings from Fig. 7(C) believed to be also present in that of Fig. 7(B) are marked with an asterisk.

C. Discussion

Comparison of the spacing data of Table 2 with those of Posnjak[6], Flörke[5], Jung[7], and Weiser *et al.*[8] indicates that the new phases observed are not those of hemihydrate, dehydrated hemihydrate (or γ–$CaSO_4$), or of gypsum. There is in general little agreement between these or most other authors either in their own experimental

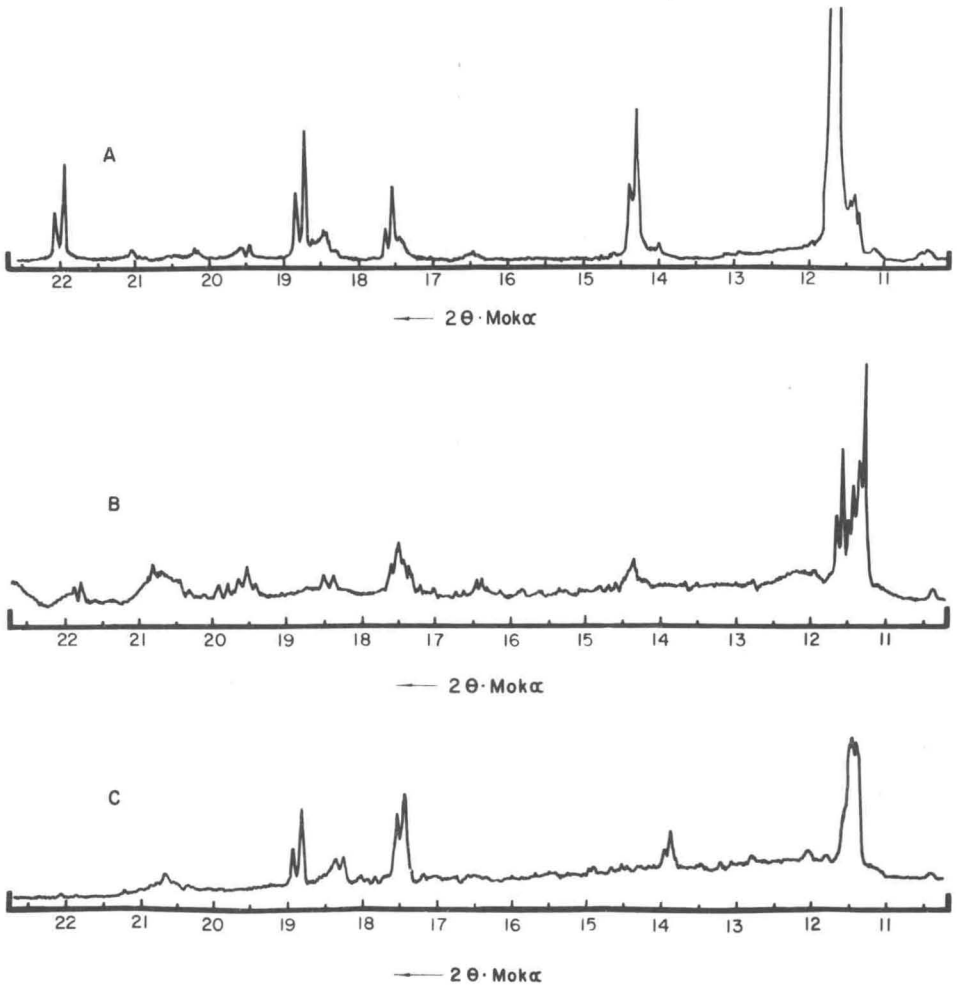

Fig. 7. (A) Standard 'well' mount X-ray diffraction pattern of anhydrite taken immediately after heating to 375 ± 25°C for 3 hr. $MoK\alpha$ radiation, 1/4 deg 2θ per min scanning speed. (B) Anhydrite plus water in X-ray vessel cycled and left at 200 bars pressure at room temperature. Same scanning conditions as in (A). (C) Anhydrite plus water in X-ray vessel cycled and left at 50 bars at room temperature. Same scanning conditions as in (A) and (B).

data or in their interpretation, but in any case the changes observed here are more obvious than those reported for the above phases. Inasmuch as they appear not to have been observed before, their existence seems dependent upon the presence of excess water and slight pressure.

In view of the probable effect of water pressures in stabilizing these phases we can examine the P–V relations for the equations

$$\underset{45{\cdot}9}{CaSO_4} + \underset{n+9}{(n+1/2)\,H_2O} \rightarrow \underset{51{\cdot}7}{CaSO_4 \cdot 1/2H_2O} + \underset{n}{nH_2O} \qquad \Delta V = -3{\cdot}2\ \text{cm}^3 \quad (2)$$

and

$$\underset{45{\cdot}9}{CaSO_4} + \underset{n+36}{(n+2)\,H_2O} \rightarrow \underset{74{\cdot}9}{CaSO_4 \cdot 2H_2O} + \underset{n}{nH_2O} \qquad \Delta V = -7{\cdot}0\ \text{cm}^3 \quad (3)$$

Table 2. Interplanare spacings and intensities observed with $CaSO_4$ in the presence of water (A) at 200 bars pressure and (B) 50 bars pressure**

	(A)			(B)	
d (Å)	I/I_0	hkl	d_{obs} (Å)	d_{calc} (Å)	I/I_0
3·92(1)	5	1 1 1	3·92	3·92	2
3·61	100	0 0 2	3·57	3·57	100
3·57(1)	50	0 2 0	3·40	3·41	5
3·52(2)	40	2 0 1	2·94	2·95	30
3·40(1)	3	2 2 0	2·340	2·346	70
2·84(2)	15	1 0 3	2·236	2·236	20
2·49(2)	10	0 3 1	2·170	2·165	80
2·351(1)	10	3 0 1	2·063	2·064	5
2·331(2)	20	1 2 3	1·868	1·870	5
2·219	5				
2·103	5	$a = 6{\cdot}46_9$Å			
2·088(2)	15	$b = 6{\cdot}81_5$Å			
2·061(1)	5	$c = 7{\cdot}14_8$Å			
1·877(3)	10				
1·672	10				
1·649	10				
1·527	15				
1·423	5				
1·400	5				
1·280	5				

*Mokα 45 kV, 20 mA, 1/8 deg min. scan speed, 1/4 deg divergence and scatter slits, 0·006 receiving slit.
(1) = observed in Table 2 (B).
(2) = anhydrite.
(3) = spacings smaller than this value may be indexed as anhydrite or distorted anhydrite.

with molar volumes of each phase, where n is added only to indicate an excess but finite quantity of water within the (closed) system. Because pressure within the system acts on all phases, the volume of water entering into the solid phases during the reaction must be taken into account.

The above relations demonstrate that at constant temperature both the hemihydrate and gypsum are stable with respect to anhydrite at moderate pressures. At higher pressures we take into account the compressibility relations for gypsum and anhydrite given by Madelung and Fuchs[9] and the equation of state for water as given by Li[10]. The molar volumes for equation (3) from left to right at 5000 bars are 45·5, 31·1 and 74·0, indicating only a slight pressure effect upon the solid phases. The volume change, however, is now $-2{\cdot}6$ cm^3, and in the vicinity of 10,000 bars volumetric equilibrium between the left and right sides of equation (3) is reached. The above relations were obtained from data of somewhat limited accuracy inasmuch as the constants for the second terms of the quadratic compression equations were not determined by Madelung and Fuchs for the two solid phases. However, inasmuch as the volume change contribution by these phases is small compared to that of water, little error will be introduced into the calculations.

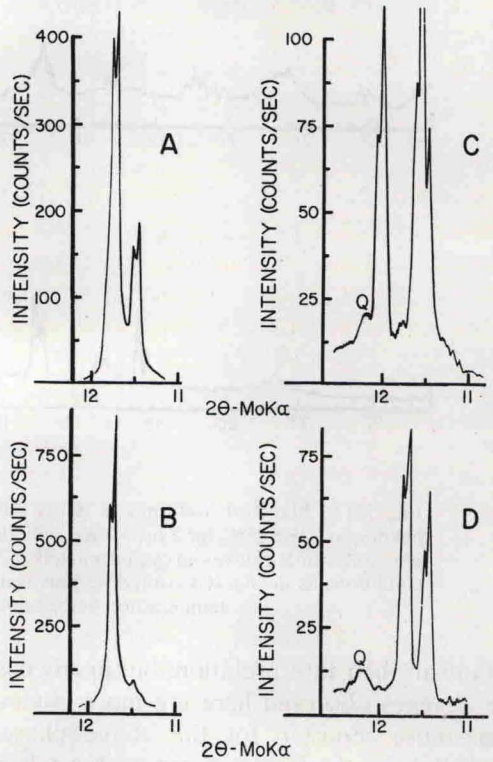

Fig. 8. (A) Peaks observed between 11 and 12 deg 2θ from natural dry anhydrite open to the atmosphere for three months. (B) Same material as in (A) above but heated 375 ± 25°C 3 hr. Standard 'well' mount. (C) Anhydrite in the presence of distilled water in X-ray vessel, showing same region as in (A) and (B). Q is peak from quartz internal standard. Pressure is 25 bars at room temperature. No pressure cycling. (D) As above except pressure raised to 1200 bars and reduced to near 1 atmosphere.

Although the observed changes in X-ray pattern are most likely due to partial hydration, neither the hemihydrate nor gypsum was formed to any degree during any of the experiments. Anhydrite plus water was pressurized at 2000 bars for several hours with no indication of transformation to gypsum. Higher pressure does not enhance the transformation as we have seen above. It seems, therefore, that the phases observed are hydration states of $CaSO_4$ where n is neither 1/2, nor 2, with complete transformation to gypsum being kinetically difficult.

The two peaks with spacings 3·57 and 3·61 Å are unique in that they may be observed in patterns of 'dry' anhydrite and are enhanced and often dominate the pattern at moderate pressures.

Figure 8 shows several tracings of the 11–12 deg 2θ region of the pattern; (A) is a pattern taken from anhydrite after 3 months open to the atmosphere showing strong development of the 3·61 Å peak. Diagram (B) shows the same material after heating for 3 hrs at 375°C. Figure 8(C) shows almost no 020–002 doublet of anhydrite but a stronger development of the 3·40 and 3·57 Å peaks observed for the new phase shown in Fig. 7(C). In this pattern a small amount of the 3·61 Å peak may be present. Figure 8(D) shows the anhydrite 020–002 doublet with the 3·61 Å peak well developed. Control for precise positions for these peaks was obtained by using a quartz internal standard.

That one of more new phases of a possible hydrated $CaSO_4$ exists under the conditions of these experiments is well demonstrated by the foregoing data. The first set of data in Table 2 contains a mixture of anhydrite peaks and those of the new phase(s) and therefore no attempt at indexing was made. However, the pattern shown in Fig. 7(C) is distinct and enough different from that of anhydrite that closer examination of these spacings is justified. The data of column(B), Table 2 do not fit those of the hemihydrate or γ-$CaSO_4$, but can be indexed easily on the basis of a distorted anhydrite cell with $a = 6{\cdot}46_9$ Å, $b = 6{\cdot}81_5$ Å, and $c = 7{\cdot}14_8$ Å. It appears that if this cell is the correct one the space group may still be B-centered but must be of lower rank than the Bbmm assigned to anhydrite proper. With the cell constants of anhydrite heated to 375°C for 3 hrs (still not completely anhydrous) as $a = 6{\cdot}19_2$ Å, $b = c = 6{\cdot}98_8$ Å, we observe 4·5 per cent expansion of the a-axis, 2·5 per cent contraction of the b-axis, and 2·3 per cent expansion of the c-axis, resulting in a cell volume *increase* of 4·6 per cent.*

Assuming then, that the distorted cell contains four formula units of $CaSO_4$, one can determine the theoretical value of n, the hydration coefficient, from a plot of n vs. volume per formula unit (V_c/Z) for the phases anhydrite, hemihydrate, and gypsum (Fig. 9). The resulting value of n for the distorted anhydrite phase is 0·167. The total molar volume change is thus given by

$$\underset{45{\cdot}9}{CaSO_4} + (n + 1/6)\underset{3{\cdot}0}{H_2O} \rightarrow \underset{47{\cdot}6}{CaSO_4 \cdot 1/6\, H_2O} + n\underset{\Delta V = -1{\cdot}3\text{cm}^3.}{H_2O} \qquad (4)$$

The above relation is not an independent test of the cell but the volume decrement is a result of the position of n on the volume plot of Fig. 9.

It is puzzling that the obvious 3·61 Å peak has not been reported in the literature (Posnjak[6], Jung[7], Weiser *et al*[8], Swanson *et al.*[11], Bunn[12]. Bunn examined material with $n = 0{\cdot}19$ but did not observe any changes in the X-ray pattern. These

*Axis orientation here is that used by Swanson *et al.*[11].

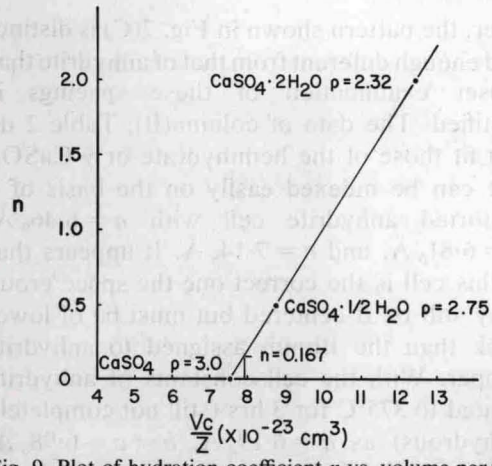

Fig. 9. Plot of hydration coefficient n vs. volume per formula unit (V_c/Z) for gypsum, hemihydrate, and anhydrite. Value of n for distorted anhydrite cell is 0·167.

facts may indicate that slight pressure, less than 100 bars, is required to form the new phase, and, although it is not significant in commercial uses of $CaSO_4$ its presence might be expected in those stratigraphic sections containing water pressures of this magnitude or higher.

Although there are good reasons for accepting the above cell type for the new phase as correct, the structural relationship to the normal anhydrite cell is not clear. One would expect, for example, that the a-axis (shortest dimension of the anhydrite structure)being that direction parallel to Ca–SO_4 'chains,' would expand less than the b or c axes, whereas b actually contracts. The drastic change in X-ray pattern, does, however, indicate marked structural changes that do not take place easily, but nevertheless are reversible. In view of the lack of the appearance of the hemihydrate in these studies a hydration state equal to $n = 1/2$ was not attained. It is thus concluded here that a definite structural state of hydration with n less than 1/2 can exist in the $CaSO_4$–H_2O system.

One notes from Table 2 (A) that not all of the spacings have been accounted for by the anhydrite and distorted anhydrite structures. The 3·61 Å peak is especially strong and seems to develop under pressures greater than that required to form the distorted phase. This and probably other of the new peaks unaccounted for may represent another hydration state, but present data are insufficient to warrant a structural investigation.

4. INVESTIGATION OF THE STABILITY OF AgI–IV

The low-pressure phase IV of AgI (also known as the 3 kbar phase) was discovered by Van Valkenburg[13] and studied further by Adams and Davis[2] and by Bassett and Takahashi[14]. There is no doubt that the phase can be formed but to date no one has established the reality of a true pressure–temperature stability field with respect to the other known polymorphs of AgI. Davis and Adams[15] suggested a positive P–T slope for the II–IV boundary [phase nomenclature is summarized by Bassett and Takahaski[14]] based on a maximum temperature for the II–III–IV triple point of about 50°C and one room temperature point in the diagram for the appearance of phase IV. Because of the slight possibility of the occurrence of phase IV in sub-zero quench products from acetone generators or pyrotechnic devices, it was considered advisable to investigate the stability region of this phase, and in particular, to plot out the II–IV stability boundary.

The same apparatus was used here as for the $CaSO_4$–H_2O experiments. Some higher temperature data were obtained using the vessel described by Adams and Davis[2] (p. 362) using cornstarch pressure medium. In addition, at the kind invitation of Van Valkenburg, one of us (B.L.D.) observed in his laboratory some pertinent high-pressure optical experiments on single crystals of AgI which will be mentioned below.

A. Results

A large number or runs from 0–30°C with pressure raised in 200 bar increments from 2000–4000 bars were performed on various types of silver iodide. In all cases, transforma-

tion to the high-pressure phases was extremely slow. This included AgI from two different chemical suppliers, from our own preparation (0·085 molal NaI solution poured into boiling 0·097 molal $AgNO_3$ solution), AgI heated overnight at 140°C, AgI passed through the II–I boundary (to aid in conversion of II′ to II), and AgI ground vigorously in a mortar (to convert II to II′).*

Several runs were made at temperatures from 30–60°C and in all cases the high pressure from created was III alone. This is in agreement with previous results of Davis and Adams[15] but not with those of Bassett and Takahashi[14], where a triple-point of $65° \pm 2°C$ was determined for II–III–IV. Transformation kinetics do not explain the discrepancy because if phase IV appears below 30°C it should certainly appear above this temperature if a true stability field for phase IV existed near the triple point.

Figure 10 presents the results of the AgI experiments. Runs at 50 and 60°C were made with cornstarch pressure medium and all others with kerosene. From the runs completed on fine-grained polycrystalline aggregates it is apparent that the II–IV boundary may exist but cannot be accurately determined with the present apparatus. Most of the data in this figure can be used only to resitrict the position of the II–III boundary within the dashed lines, inasmuch as the growth of phases were not observed, but only the presence of certain phases after a period of time for growth had elapsed.

These boundaries represent 30 min isocrons† for about 20 per cent conversion; that is, the transformation rate was sufficiently great to accomplish about 20 per cent conversion to the new phase in 30 min, the duration of most experiments. Several long-period experiments, lasting up to 24 hrs, demonstrated that phase III grew along with phase IV at the expense of phase II + II′ at 25°C and 3350 bars, and that phase II′ + II grew at the expense of III and IV at 2800 bars. Again, on the up-pressure leg of the run, phase IV appeared at precisely the same time as phase III and remained with phase III as both inverted to II + II′ at 2800 bars.

The long period experiment at 2800 bars (station 1, Fig. 10) shows that the II–III boundary lies closer to the +30 min isocron. Further positioning of this boundary between stations 1 and 2 is arbitrary because these points do not lie on equal but opposite isocrons, nor was the exact amount of conversion determined for the runs. By placing this boundary midway between the stations, and taking the boundary slope to be the average of the isocron slopes, the boundary lies 90 bars above that originally determined by Bridgman[17] for the II–III stability fields, with a slope of −0·56 deg/bar, compared to −0·42 given by Bridgman. Even with the uncertainties occasioned by the sluggishness of inversion, the boundary at 30°C can be no higher than 3350 bars, no lower than 2800 bars, and is given here as 3100 bars.

B. Discussion

Many unsuccessful attempts were made to convert AgI II + II′ to IV (for times up to 8 hrs) with fine powders of silver iodide in the above manner. Then Van Valkenburg (personal communication) noted that single crystals of hexagonal AgI (II) (some of which were as small as the coarse fraction of the powders used here) transformed under pure hydrostatic pressure to AgI–IV quickly and without polygonization. We therefore attempted another X-ray run with coarse powder (about 50 μ), also pure phase II. By increasing the pressure at small increments in the 2800–3200 bar region it was possible to convert most of this originally phase II material into phase IV. The optical experiments performed in Van Valkenburg's laboratory, which were observed by one of us (B.L.D.), demonstrated conclusively that

*For the effects of grinding of the stability of the II and II′ phases, see Burley[16].

†Time isolines.

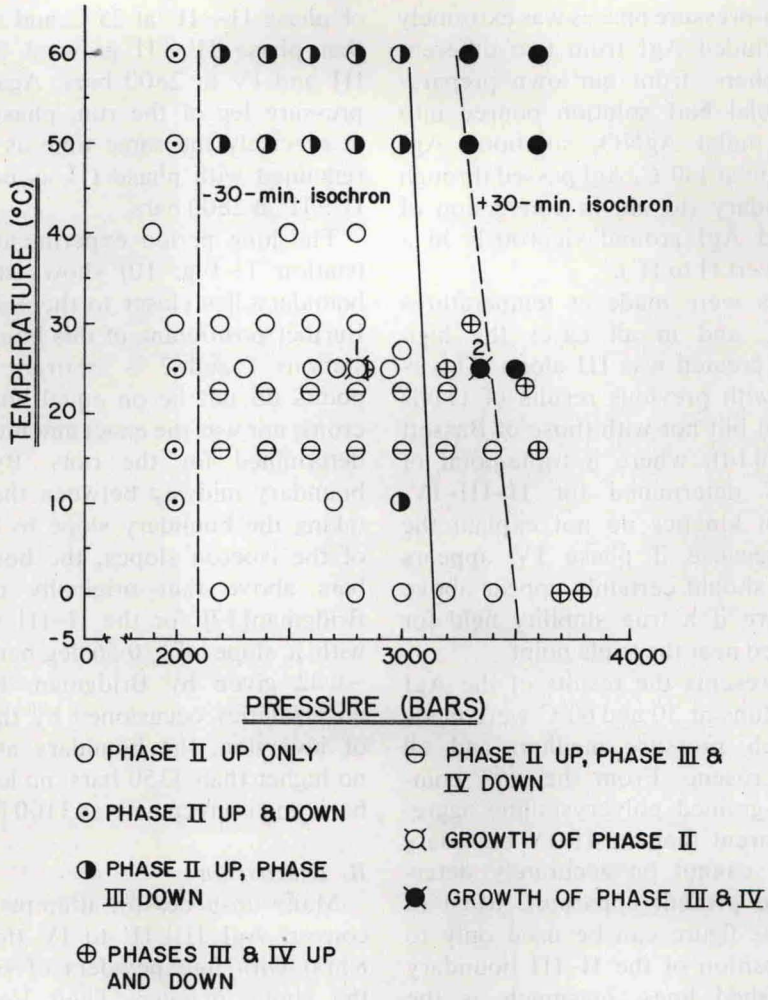

Fig. 10. Observed phase relations for AgI in the II, III, and IV regions. Solid line is estimated II–III boundary. See text for further explanation.

small single grains of hexagonal silver iodide could be converted readily into phase IV. There appear to be no polygonization during this process unless the phase III region was entered and phase III formed.

In view of the X-ray experiments on the coarse powder, and the optical experiments, it appears that the width of the phase IV stability region at room temperature can be no greater than 50 ± 25 bars. It is also becoming more apparent from further X-ray data taken in this laboratory and from the nature of the II–IV transformation observed optically that there is a close structural relationship between these two phases. Such a relationship was noted to exist in indexing of phases II and IV by Davis and Adams [15].

One of the prime purposes of this investigation was to see if AgI–IV could occur in the atmosphere under quenching conditions from silver iodide generators. It now appears that such a condition would be highly improbable from the following viewpoints:

1. Assuming the correctness of the boundary separating phases II from III, as established by Bridgman [17] and by the results shown in Fig. 10 of this paper, and that the width of the phase IV field is less than 100 bars as sugested above, he supposed but unplotted phase II–IV boundary would be vertical or very steep and would plot at about 3000 bars at room temperature. Such a boundary would not extrapolate to natural environmental temperatures (warmer than −60°C) at atmospheric pressure.
2. The present data indicates that the cubic form of AgI (II′) will not transform to phase IV. All runs of fine-grained AgI contained some phase II′ (cubic) as well as II (hexagonal) and only partial conversion to phase IV was accomplished. Large solution-grown hexagonal crystals were used in the optical and coarse-grain X-ray runs where nearly complete to complete transformation was accomplished. Under these conditions very little phase IV could form in natural aerosols even if the II stability was appropriate because AgI generator output is primarily cubic AgI (II′) (a fact verified in this laboratory).

Figure 10 gives us some information about the rate constants for the forward and reverse process in the II to III transformation. If the rates for each process were identical, the phase boundary would fall exactly halfway between the +30 min 20 per cent isocron and the −30 min 20 per cent isocron. In view of the position shifted toward the +30 min 20 per cent isocron, it follows that the forward process (conversion to III) is more rapid than the reverse. Because this phenomenon is present at higher temperatures as well as below 30°C, the rate difference must be due to different II–III activation states rather than to the presence of phase IV.

Acknowledgements—The studies in the system $CaSO_4$–H_2O were supported by the National Science Foundation (GP5075), and the work on the AgI phase relations by the Office of Atmospheric Water Resources, Bureau of Reclamation, Contract No. 14-06-D-5979.

REFERENCES

1. KELMENT W. Jr., and JAYARMAN A., *Prog. solid State Chem.* **3**, 289 (1966).
2. ADAMS L. H. and DAVIS B. L., *Am. J. Sci.* **263**, 359 (1965).
3. SLATER J. C., *Phys. Rev.* **23**, 488 (1924).
4. DEER W. A., HOWIE R. A. and ZUSSMAN J., *Rock Forming Minerals*. Wiley, New York (1962).
5. FLÖRKE O. W., *Neues J. Miner. Ab.* **84**, 189 (1952).
6. POSNJAK E., *Am. J. Sci. (ser. 5)* **35A**, 247 (1938).
7. JUNG H., *Z. anorg. allg. Chem.* **142**, 73 (1925).
8. WEISER H. B., MILLIGAN W. O. and ECKHOLM W. C., *J. Am. chem. Soc.* **58**, 1261 (1936).
9. MADELUNG E. and FUCHS R., *Annln. Phys.* **65**, 289 (1921).
10. Li Y., *J. geophys. Res.* **72**, 2665 (1967).
11. SWANSON H. E. FUYAT R. K. and UGRINIC G. M., *Standard X-ray Diffraction Patterns. Nat. Bur. Stds. Circ. 539 IV*, p. 65 (1955).
12. BUNN C. W., *J. scient. Instrum.* **18**, 72 (1941).
13. VAN VALKENBURG A., *J. Res. Nat. Bur. Stand.* **68A**, 97 (1964).
14. BASSETT W. and TAKAHASHI T., *Am. Mineral.* **50**, 1576 (1965).
15. DAVIS B. L. and ADAMS L. H., *Science* **146**, 519 (1964).
16. BURLEY G., *J. phys. Chem.* **68**, 1111 (1964).
17. BRIDGMAN P. W., *Am. Acad. Arts Sci.* **51**, 55 (1915).